A Tail of Four Fishes: An analysis of kinematics and material properties of elongate fishes

Lydia F. Naughton[1]*, Sebastian Kruppert[2], Beverly Jackson[3], Marianne E. Porter[4], Cassandra M. Donatelli[5]

*corresponding author
[1]Bucknell University; 701 Moore Ave, Lewisburg PA, 17837; lfn001@bucknell.edu; 443-886-4607
[2]University of Washington, Friday Harbor Labs; sebastian.kruppert@googlemail.com
[3]Idaho State University; beverlyjackson@isu.edu
[4]Florida Atlantic University, Biological Sciences; mporte26@fau.edu
[5]University of Ottawa, Department of Biology; cdonatel@uottawa.ca

Running Title: Fish mechanics tuned to habitat and diet

Abstract

The elongate body plan is present in many groups of fishes, and this morphology dictates functional consequences seen in swimming behavior. Previous work has shown that increasing the number of vertebrae, or decreasing the intervertebral joint length, in a fixed length artificial system increases stiffness. Tails with increased stiffness can generate more power from tail beats, resulting in an increased mean swimming speed. This demonstrates the impacts of morphology on both material properties and kinematics, establishing mechanisms for form contributing to function. Here, we wanted to investigate relationships between form and ecological function, such as differences in dietary strategies and habitat preferences among fish species. This study aims to characterize and compare the kinematics, material properties, and vertebral morphology of four species of elongate fishes: *Anoplarchus insignis, Anoplarchus purpurescens, Xiphister atropurpureus,* and *Xiphister mucosus*. We hypothesized that these properties would differ among the four species due to their differential ecological niches. To calculate kinematic variables, we filmed these fishes swimming volitionally. We also measured body stiffness by bending the abdominal and tail regions of sacrificed individuals in different stages of dissection (whole body, removed skin, removed muscle). Finally, we counted the number of vertebrae from CT scans of each species to quantify vertebral morphology. Principal component and linear discriminant analyses suggested that the elongate fish species can be distinguished from one another by their material properties, morphology, and swimming kinematics. With this information combined, we can draw connections between the physical properties of the fishes and their ecological niches.

Introduction

The elongate body plan has evolved many times across the fish tree of life (Claverie and Wainwright, 2014; Mehta et al., 2010). Many elongate fishes swim using an undulatory gait, in which the bending body generates waves that propagate from anterior to posterior and propel the fish forward (Long et al., 1994). Though there is some variation in the undulatory wave, such as the percentage of the body used, the general kinematics typically follow established patterns. For fishes in general, swimming speed is often directly proportional to tail beat frequency, whereas tail beat amplitude generally stays the same across speeds (Bainbridge, 1958). Elongate fishes use an extreme form of undulatory kinematics often referred to as anguilliform swimming. In anguilliform swimming, elongate fishes take advantage of their highly flexible bodies to pass a bending wave of increasing amplitude from their heads to their tails (Sfakiotakis et al., 1999; Tytell, 2004). In elongate fishes, this form of locomotion is 4-6 times more efficient than non-elongated fishes and has been hypothesized to be a major factor which allows migratory species, such as European Eels (*Anguilla anguilla*), to swim 5000-6000 km without eating (van Ginneken et al., 2005).

In addition to kinematics, the material properties of the fish body and of individual tissues are also known to affect swimming behavior (Donatelli et al., 2017; Long et al., 1996; Nowroozi and Brainerd, 2014; Porter et al., 2014; Wainwright et al., 1978). The three main material components considered in this study are skin, muscle, and bone. Each of these materials contributes to the overall flexibility and swimming attributes of the fish (Altringham and Ellerby, 1999; Hirokawa et al., 2011; Long et al., 1996). Long et al. (1996) investigated the effects of body mechanics on swimming kinematics by removing the dermal scales of the longnose gar, reducing its overall bending stiffness. They found that when the skin is removed from the fish, tail beat frequency decreased and tail amplitude increased (Long et al., 1996). In this case, without the supporting structure of the skin, the fish must alter its swimming behavior to account for increased flexibility. Simulations have also demonstrated the impact of stiffness on fish swimming kinematics: Tytell et al. (2010) developed a computational model of lamprey swimming that considered body stiffness, muscle activation, and hydrodynamics. This model showed that, for a given muscle activation pattern, low body stiffness yielded higher mean acceleration but slower steady swimming speed compared to high body stiffness (Tytell et al., 2010). In addition to *in vivo* experiments and simulations, material testing experiments have provided much insight into the biomechanics of fishes. Long and colleagues quantified the stiffness provided by multiple body materials for the hagfish. They sequentially removed the skin, muscle, and notochord sheath from euthanized hagfishes and measured the strain on the body during bending. Both the muscle and the notochord sheath were significant contributors to stiffness (Long et al., 2002).

Bony vertebrae, which are an important component of the body plan for most vertebrate fishes, were not quantified in previous experiments. One morphological characteristic of the vertebral column that has implications for material stiffness and kinematics is the presence of bony centra (Donatelli and Porter, 2013; Long et al., 1997; Nowroozi et al., 2012). During development, the ossification of the centra obliterates the notochord and gives rise to the formation of the vertebral column (Schaeffer, 1967). Centra morphology is known to affect the material properties of the entire vertebral column. For example, by adding artificially designed centra to a model hagfish notochord, Long et al. (2004) found that, as intervertebral joint length increased, the stiffness of the notochord decreased (Long et al., 2004). Long and colleagues also built a mobile autonomous robot (TADRO) for mechanical testing with biomimetic vertebral columns to quantify the effects of vertebral count on stiffness and swimming behavior (Hirokawa et al., 2011). They created several models with a range of vertebral densities and measured swimming performance in a bioinspired robot. This study showed that tails with increased stiffness, i.e., higher vertebral density, had greater peak acceleration and mean swimming speed (Long et al., 2011). The findings from these studies suggest that as fishes evolved elongated body plans, the total number of vertebrae may have increased, rather than the length of a set number of vertebrae, in order to conserve local body stiffness. In fact, elongation in actinopterygian fishes is most strongly associated with an increase in vertebral number, as opposed to an increase in aspect ratio of the vertebrae, and generally, the increase is greater in the tail region compared to the abdominal region (Mehta et al., 2010; Ward and Brainerd, 2007).

Though all these studies investigate effects of individual morphological components on locomotion, very few integrate gross morphology, mechanics, kinematics, and ecology. We are curious about the material contributions of body tissues and morphology on behavior, especially swimming kinematics, in species with varying ecological niches. In order to investigate this, we chose to examine four species of fishes from the family Stichaeidae: *Anoplarchus insignis, Anoplarchus purpurescens, Xiphister atropurpureus,* and *Xiphister mucosus*. These four fishes all reside in and near the rocky intertidal zone in the Pacific Northwest. They are all benthic fishes that tend to situate themselves beside and underneath rocks, but they each occupy slightly different ecological niches. *A.insignis* and *X.atropurpureus*, for example, tend to live several meters deeper than the other two species (Froese and Pauly, 2019; Lamb and Edgell, 2010). In terms of diet, both *Anoplarchus* species are carnivores, *X. atropurpureus* is an omnivore, and *X. mucosus* is an herbivore (German et al., 2015).

Using these fishes, our goal was to answer the following questions. 1) How do tail amplitude, head amplitude, and tailbeat frequency change with swimming speed? Based on previous work, we predict that tail and head amplitude will not change with swimming speed while tailbeat frequency will increase as speed increases. 2) Which body tissues (skin, muscle, or vertebral column) contribute the most to stiffness? Due to the stiffness of bone at the tissue level and previous documented impacts of vertebral column mechanics on swimming, we predicted that the vertebral column would have the greatest impact on body stiffness. 3) Do body mechanics and vertebral morphology impact swimming kinematics? We expected that swimming speed would be tied with vertebral counts and body stiffness, especially vertebral column stiffness. 4) When examining the suite of variables quantified here, can we draw connections between the combined variables and the ecological niches that these four fishes occupy? With the kinematics, material properties, and morphometrics data, we aimed to explain the ecological differences, such as dietary strategy and habitat preference, among our four fishes.

Materials and Methods

Specimen Collection and Care. We collected five individuals each of four species of fishes from the family Stichaeidae: *Anoplarchus purpurescens, Anoplarchus insignis, Xiphister atropurpureus,* and *Xiphister mucosus* (Figure 1). We caught these fishes by flipping over rocks and scooping them out of tidepools during low tide at Friday Harbor Laboratories and Deadman's Bay in San Juan Island, Washington, USA. Specimens ranged in size from 8 cm to 25 cm (Table 1). We housed fishes in open sea tables fed from a flow through system. The specimens were sacrificed prior to material testing using a lethal dose of MS222 following IACUC protocol 4238-03.

Kinematic Analysis. In order to understand the swimming kinematics of the elongate fishes, a video recording setup was designed to record their movement (Figure 2). A long, rounded track was placed in a 1.425 m x 0.61 m x 0.14 m tank so that each fish could circle the tank and cross through the video frame at its own pace. The device used to record videos was a GoPro Hero4 (GoPro Inc, San Mateo CA, USA) with settings set to 1080p resolution, 30 frames per second, and a linear field of view. In a GoPro, the linear field of view corrects the distortion from the fisheye lens. Five individuals of each species were filmed, and 5-11 steady swimming trial video clips were collected for each individual. We considered a swimming bout "steady" if the animal did not appear to accelerate or decelerate during the bout. Videos were trimmed to the duration that included the behavior of interest using MPEG Streamclip (Squared 5 srl, Rome, Italy). We used a custom Matlab code to track the midlines of the five cleanest videos for each individual (Matlab R2020a, Mathworks, Natik MA, USA) (Donatelli et al., 2017). We used another Matlab script to calculate swimming speed (BL-body lengths-per second), tail beat frequency (Hz), tail beat period (s), stride length (BL), tail beat amplitude (BL), head amplitude (BL), and body amplitude (BL) at three points along the midline (25%, 50%, and 75% posterior from the head). These kinematic data points were formatted into a table and imported into R for statistical analysis (R version 4.0.1; RStudio Desktop 1.3.1073, Boston, MA, USA).

Material Testing. We used an MTS Synergie 100 material tester (MTS Systems Corp, Eden Prairie, MN, USA) to measure the mechanical properties of different components of fish bodies (Figure 3A). Individuals (N=2 for *A. insignis*, N=3 for the three other species) were placed in a tank with 4 L of seawater and 1 g of MS-222 for 60 minutes to be sacrificed following IACUC protocol 4238-03. Specimens were then sealed in bags and left in the freezer until needed for material testing within the next 6 days. Once the specimens underwent one freeze-thaw cycle, the fishes were tested under three different conditions: 1) fully intact (Figure 3B), 2) skin removed (Figure 3C), and 3) muscle removed (Figure 3D). For the second condition, the skin was peeled off of the fish from the back of the head down to the caudal fin. The abdominal cavity was cleared to avoid leakage during the bending trials. For the third condition, the bulk of the muscle was scraped off over the same length of the fish as the previous dissection. Only the vertebral column and a thin layer of muscle and connective tissue between the spines were left intact.

After each dissection, the fish was bent in two different regions along the body: the abdomen and the tail (Figure 3E). The abdomen was defined as the length between the end of the head and the beginning of the anal fin; the tail was defined as the length between the beginning of the anal fin and the beginning of the caudal fin. When testing the bending performance of the abdomen, the stationary gripper and the pulling string were attached inward of the head and anal fin by 10% of the abdomen length. For the tail bending trials, the stationary gripper and the pulling string were attached inward of the anal fin and the tail fin by 10% of the tail length. In both trial types, the point of the string attachment was aligned with the material tester pulley so that the string was pulling perpendicular to the body (Figure 3A).

The fish was placed on a thin wooden board with a protractor taped to it. A single bending test started when the 500 N load cell began to rise, pulling the string and bending the specimen. The test terminated when the specimen reached its maximum bending angle - a switch from bending to tensile mode. The material tester measured the force (N) exerted on the fish during bending and the linear distance the string traveled (mm).

The bending trials were filmed using a Nikon D5300 (1920x10180, 60p, Nikon Inc, Minato City, Tokyo, Japan) to provide a visual record of each test. We then analyzed these videos using the Matlab app DLTdv8 (DLTdv8a version 8.2.0) (Hedrick, 2008) to track two points frame by frame on the fish body as it bent: the bending point and the anchor point. The bending point was marked at the site of string attachment, and the anchor point was marked at the stationary gripper. The program recorded the x-y coordinates for each point for every frame, so we then calculated the angle between the two points over all frames for each video.

Morphometrics. We counted the total number of vertebrae down the length of the body in our species using CT scans of the specimens. We got scans of our four species from the Scan All Fishes and oVert projects (Watkins-Colwell et al., 2018). The vertebrae of each of our fish were marked in 3D Slicer following the protocol from Buser et al (2020) and we extracted the coordinates for measurement in Matlab (Buser et al., 2020; BWH and Contributors, 2019).

Statistical analysis. We compiled our kinematics, mechanics, and morphometrics into csv files and imported them into R for statistical analysis. To analyze the kinematics data, we created linear models to ask if tail beat amplitude, head amplitude, and tail beat frequency were affected by swimming speed (Figure 4). For the material testing data, we examined variations of both abdominal stiffness and tail stiffness by species and dissection condition using a chi-square test. We then used pairwise t-tests to examine differences in the stiffness measurements between the three dissection conditions for each species. *A. insignis* was not included in the statistical analysis for material testing, as there were only two individuals tested. The kinematics and mechanics data were merged in R and we performed both a linear discriminant analysis (*lda()*, "MASS" package) to determine if our species could be grouped and a principal components analysis (*prcomp()*, "FactoMineR" package) to determine which factors contributed most to the variation in our data. We also excluded *A. insignis* from our LD analysis. Finally, we used the *Anova()* function ("car" package) to examine the effects of material properties (intact, muscle only, and bone only stiffness) on kinematics (swimming speed, frequency, body amplitude, and tail amplitude).

Results

The data extracted from the live swimming trials was consistent with undulatory swimming patterns typical for elongate fishes. By allowing the specimens to swim at their own pace, we were able to measure the effect of varying swimming speed on the bending wave properties of natural swimming behavior. Differences in swimming speed had no effect on head amplitude or tail beat amplitude, except for *A. purpurescens*, which displayed a significant inverse relationship between swimming speed and both tail beat amplitude and head amplitude (Figure 4A: p=0.008, R^2=0.788; Figure 4B: p=0.049, R^2=0.573). Head amplitude had a much lower maximum value at 0.032 body lengths (BL) as opposed to tail beat amplitude which had a maximum value at 0.124 BL. Conversely, swimming speed and tail beat frequency exhibited a significant directly proportional relationship for all species (Figure 4C: *X. mucosus*

212 p=0.003, R^2=0.523; *A. insignis* p=0.003, R^2=0.654; *X. atropurpureus* p<0.001, R^2=0.7664; *A. purpurescens* p<0.001, R^2=0.906). When comparing the kinematic data between each of the four species, *X. mucosus* displays the steepest linear trend line slope, and this species has the slowest maximum swimming speed at about 2 BL/s.

Abdominal stiffness and tail stiffness were examined in regards to species and to dissection condition using the material testing data (Figure 5A and B). Species was not a significant factor in determining abdominal stiffness or tail stiffness (p=0.616, p=0.425). The dissection condition, however, showed statistical significance in determining both abdominal stiffness and tail stiffness (p<0.001, p=0.036). For abdominal stiffness, there was a significant difference between the intact and vertebrae exposed conditions for *X. atropurpureus* (p=0.002) and *X. mucosus* (p=0.003). Furthermore, *X. atropurpureus* (p=0.021) and *X. mucosus* (p=0.003) showed a significant difference between the intact and muscle exposed conditions (Figure 5A). For tail stiffness, there was only a significant difference between the intact and vertebrae conditions for *X. atropurpureus* (p=0.034; Figure 5B).

The combination of material properties and kinematics quantified here showed differences between the four different species. The principal components analysis plot showed that the four species groups separated from each other (Figure 6A). We found that the first PC axis described 49.2% of the variation and was mostly weighted by kinematics variables and vertebrae count. The second PC described 20.1% of the variation and was mostly weighted by material properties. For our linear discriminant analysis (Figure 6B), the first LD axis described 89.71% of the between group variation and was weighted mostly by differences in stride length and swim speed. The second LD axis described 10.29% of the variation and was mostly weighted by swim speed, tail beat frequency, and body amplitude (Table 3).

Discussion

The four species of elongate fishes examined in this study have interesting differences in material properties, vertebral morphology, and swimming kinematics. The two *Anoplarchus* species showed a close grouping in the principal components analysis while the two *Xiphister* species displayed less overlap with each other. *X. mucosus* grouped the furthest to the right along the PC1 axis (Figure 6A). This could be a result of each of their ecological niches. The two *Anoplarchus* species are both carnivores, which might explain their similar kinematic, morphological, and material properties. The *Xiphister* species, on the other hand, do not share the same diet; *X. atropurpureus* is an omnivore and *X. mucosus* is an herbivore. *X. mucosus* could be the most distinguished of all of the groups along the PC1 axis because they are the only species that do not actively hunt for prey items. In the linear discriminant analysis, the three species separate well across LD1 while the *Xiphister* species further separate from *A. purpurescens* along LD2 (Figure 6B). Interestingly, *A. purpurescens* and *X. atropurpureus* are close together along LD1 which could be explained by an overlap in their diet.

From our kinematics plots, we can see that the less intertidal species, *A. insignis,* and *X. atropurpureus*, have more similar kinematics than the other two, more intertidal species. Species that tend to live *near* the intertidal zone do not regularly deal with the constantly changing conditions of living *in* the intertidal zone. The preference of deeper habitats is equal to an avoidance of the intertidal and its complexity. It is safe to assume that species movement performances match the preferred habitat complexity, and thus, species with similar habitat preference are more likely to share kinematic and morphological characteristics than species with different preferences.

The material properties of the fishes, specifically the stiffnesses of the abdomen and the tail, were affected by sequential removal of the skin and muscle. When comparing the two body regions, the dissection condition had a greater effect on the abdominal stiffness than on tail stiffness (Figure 5). This result has two significant implications. First, because locomotion-generating waves originate near the front of the body and propagate backward, higher stiffness would be needed in the abdominal region to produce waves (Long et al., 1994). The skin and muscle of the abdomen could therefore be primarily responsible for this region's rigidity for the purpose of generating power for these traveling waves. Second, while the abdominal region is thicker and more dependent on the bulk of muscle and skin for stiffness, the tail is thinner and may depend more on the properties of the bone for stiffness. The assumption that it is possible to estimate tail stiffness based on bone stiffness can be applied to the modeling of thin biomaterials. Future work could focus on creating a model for approximating the stiffness of thin organisms (*Ptilicthys goodei*, for example) using the material properties of the vertebral column.

Consistent with the results from the principal components analysis, *X. mucosus* stood apart from the other three species in the material testing trials (Figure 5). One noteworthy difference in the material properties of *X. mucosus* was the change in abdominal stiffness between the intact and muscle conditions. *X. mucosus* exhibited the most significant reduction in abdominal stiffness after the skin was removed compared to the other three species. As mentioned previously, both *Anoplarchus* species are carnivores and *X. atropurpureus* is an omnivore, so all three of these fishes must partake in some degree of hunting behavior. These hunters would want to invest stiffness properties into the muscle as opposed to the skin because the muscle could exert finer control in stiffness changes (i.e. when to be stiff versus flexible) in order to quickly and efficiently pursue and catch prey items. It is therefore logical that the three hunters do not exhibit a significant decrease in abdominal stiffness when the skin is removed but do exhibit a significant reduction in abdominal stiffness from the intact condition to when the muscle is removed. It is worth mentioning that there is some variation in the material testing data (Figure 5). Though we corrected for bending angle in our stiffness calculations, a potential reason for the variation in these data is that there was not a programmed endpoint for the MTS trials, but rather a manual endpoint based on visual criteria.

The swimming properties of the four elongate fishes aligned with typical kinematic trends; however, there was some interesting variation among the species (Figure 4). Overall, both head amplitude and tail amplitude had no significant relationship to swimming speed (except in *A. purpurescens*) while tail beat frequency was directly proportional to swimming speed. Of the four species, *X. mucosus* displayed some distinctive kinematic properties. While the linear regression lines for *X. mucosus* extended along the x-axis past 3 BL/s, the maximum swimming speed recorded for this species was only 2 BL/s. This slow swimming speed maximum fits in the ecological context for *X. mucosus* because herbivores do not need to chase after their food, and therefore do not often engage in aggressive and bold swimming behaviors. This behavioral predisposition could manifest in “casual” swimming properties such as slow swimming speed and large wave amplitude. While the differences in the swimming kinematics for *X. mucosus* can be explained neatly by their outlying ecology, the difference in size of the fishes is another possible explanation for these results. Since the *X. mucosus* specimens extended to a larger length for their size range, it is possible that their larger sizes could explain why they are differentiated from the other species in regards to tail beat frequency. As fish size increases, the slope of the tail beat frequency to swimming speed ratio increases, so this might also explain why *X. mucosus* exhibits the greatest rate of change for tail beat frequency (Bainbridge, 1958).

There are a few interesting factors that could additionally affect swimming kinematics that we did not measure in this study but would like to address. Two morphological characteristics that differ across the four fishes are head shape and fin shape. Firstly, the heads of the *Xiphister* fishes appear more oblong, whereas the heads of the *Anoplarchus* fishes tend to be larger and rounder. A larger head would be heavier and lead to more drag force (Van Wassenbergh et al., 2015), so we might expect a reduced kinematic range for the *Anoplarchus* species, which we do not see (Figure 4). This could mean either that their head width has a negligible effect on their kinematics, or that there is an effect on kinematics from being carnivores. As carnivores, the *Anoplarchus* fishes may need to push their bodies a little harder to catch prey and are therefore used to swimming at a wide range of speeds, despite the effect of their large head. Because we did not measure head morphology or the kinematics of feeding behavior, we cannot make a conclusion either way, but we believe that these are interesting factors to consider. Fin shape is another factor that could potentially affect swimming kinematics. The pectoral fins for all four species are quite small, but the *Anoplarchus* fins are more prominent. The fishes rest on their pectoral fins when sitting on the substrate (Figure 1) but tend to tuck them to their sides during swimming, so they are unlikely to have an effect. The dorsal fin, however, is a bit taller in the *Anoplachus* species than it is in the *Xiphister* species, so it could have an effect on the kinematics by creating a larger hydrofoil and increasing thrust at the caudal fin (Han et al., 2020). In that case, we may expect *Anoplarchus* to out-perform *Xiphister*. Though we did not measure performance directly, we can say that all four species choose to swim at close to the same range of speeds when corrected for body length. The dorsal fin-vertebral connection could be a fascinating avenue for further exploration. Because the *Anoplarchus* species have bigger heads, making their swimming potentially less efficient, but also larger fins, making them theoretically more efficient, we speculate that these two factors may be leveling out their swimming performance.

This study combined kinematic, biomechanical, and morphological data to establish a relationship among four different species of elongate fishes. Our analysis showed that each species has a unique combination of mechanical properties and kinematic preferences. With this information, we were able to draw connections between the physical properties of the fish and their ecological niches. The herbivorous *X. mucosus* was separated from the other three carnivorous species, and the deeper dwelling *A. insignis* and *X. atropurpureus* separated from the other two species. These findings reinforce the thematic connection between form and function in nature.

Acknowledgements

The authors want to thank the NSF REU-Blinks Internship Program at Friday Harbor Laboratories for funding this research. All authors are grateful to Stacy Farina and Adam

Summers; had it not been for their outstanding efforts, the program could not have been possible. Special thanks to all of the mentors, interns, facilities staff, graduate students, and all of the FHL community for your support. S.K: further wants to thank the DFG (German Science Foundation) for funding (409126405). MEP is supported by a grant from the National Science Foundation (OS-1941713).

Data Availability: *The data underlying this article will be shared on reasonable request to the corresponding author.*

References

Altringham, J. D. and Ellerby, D. J. (1999). Fish swimming: Patterns in muscle function. *J. Exp. Biol.* **202**, 3397–3403.

Bainbridge, B. Y. R. (1958). The Speed of Swimming of Fish as Related to Size and to the Frequency and Amplitude of the Tail Beat. *J. Exp. Biol.* **35**, 109–133.

Buser, T. J., Boyd, O. F., Cortés, Á., Donatelli, C. M., Kolmann, M. A., Luparell, J. L., Pfeiffenberger, J. A., Sidlauskas, B. L. and Summers, A. P. (2020). The Natural Historian's Guide to the CT Galaxy: Step-by-Step Instructions for Preparing and Analyzing Computed Tomographic (CT) Data Using Cross-Platform, Open Access Software. *Integr. Org. Biol.* **2**,.

BWH and Contributors, 3D Slicer (2019). 3DSlicer.

Claverie, T. and Wainwright, P. C. (2014). A morphospace for reef fishes: Elongation is the dominant axis of body shape evolution. *PLoS One* **9**,.

Donatelli, C. M. and Porter, M. E. (2013). Bent out of shape: Bioinspired vertebral column morphology and mechanics.

Donatelli, C. M., Summers, A. P. and Tytell, E. D. (2017). Characterizing body twisting in elongate fishes: kinematics, mechanics, and control. In *INTEGRATIVE AND COMPARATIVE BIOLOGY*, pp. E247--E247.

Froese, R. and Pauly, D. (2019). FishBase. *World Wide Web Electron. Publ.*

German, D. P., Sung, A., Jhaveri, P. and Agnihotri, R. (2015). More than one way to be an herbivore : convergent evolution of herbivory using different digestive strategies in prickleback fishes (Stichaeidae). *Zoology* **118**, 161–170.

Han, P. (韩攀), Lauder, G. V., and Dong, H. (董海波). (2020). Hydrodynamics of median-fin interactions in fish-like locomotion: Effects of fin shape and movement. *Physics of Fluids* **32**, 011902.

Hedrick, T. L. (2008). Software techniques for two- and three-dimensional kinematic measurements of biological and biomimetic systems. *Bioinspir. Biomim.* **3**, 034001.

Hirokawa, J., de Leeuw, J., Krenitsky, N. M., Porter, M. E., Long, J. H. and Roberts, S. F. (2011). Testing Biomimetic Structures in Bioinspired Robots: How Vertebrae Control the Stiffness of the Body and the Behavior of Fish-Like Swimmers. *Integr. Comp. Biol.* **51**, 158–175.

Lamb, A. and Edgell, P. (2010). *Coastal Fishes of the Pacific Northwest*. 2nd ed. (ed. Robson, P.) Maderia Park, BC: Harbour Publishing.

Long, J. H., Mchenry and Boetticher (1994). Undulatory Swimming: How Traveling Waves Are Produced and Modulated in Sunfish (Lepomis Gibbosus). *J. Exp. Biol.* **192**, 129–45.

Long, J. H., Hale, M. E., Mchenry, M. J. and Westneat, M. W. (1996). Functions of fish skin: Flexural stiffness and steady swimming of longnose gar Lepisosteus osseus. *J. Exp. Biol.*

199, 2139–2151.

Long, J. H., Pabst, D. A., Shepherd, W. R. and McLellan, W. A. (1997). Locomotor design of dolphin vertebral columns: Bending mechanics and morphology of Delphinus delphis. *J. Exp. Biol.* **200**, 65–81.

Long, J. H., Koob-Emunds, M., Sinwell, B. and Koob, T. J. (2002). The notochord of hagfish Myxine glutinosa: visco-elastic properties and mechanical functions during steady swimming. *J. Exp. Biol.* **205**, 3819–3831.

Long, J. H., Koob-Emunds, M. and Koob, T. J. (2004). The mechanical consequences of vertebral centra. *Bull Mt Desert Isl. Biol Lab* **43**, 99–101.

Mehta, R. S., Ward, A. B., Alfaro, M. E. and Wainwright, P. C. (2010). Elongation of the body in Eels. *Integr. Comp. Biol.* **50**, 1091–1105.

Nowroozi, B. N. and Brainerd, E. L. (2014). Importance of mechanics and kinematics in determining the stiffness contribution of the vertebral column during body-caudal-fin swimming in fishes. *Zoology* **117**, 28–35.

Nowroozi, B. N., Harper, C. J., De Kegel, B., Adriaens, D. and Brainerd, E. L. (2012). Regional variation in morphology of vertebral centra and intervertebral joints in striped bass, Morone saxatilis. *J. Morphol.* **273**, 441–452.

Porter, M. E., Diaz, C., Sturm, J. J., Grotmol, S., Summers, A. P. and Long, J. H. (2014). Built for speed: Strain in the cartilaginous vertebral columns of sharks. *Zoology* **117**, 19–27.

Schaeffer, B. (1967). Osteichthyan vertebrae. *Zool. J. Linn. Soc.* **47**, 185–195.

Sfakiotakis, M., Lane, D. M. and Davies, J. B. C. (1999). Review of fish swimming modes for aquatic locomotion. *IEEE J. Ocean. Eng.* **24**, 237–252.

Tytell, E. D. (2004). The hydrodynamics of eel swimming II. Effect of swimming speed. *J. Exp. Biol.* **207**, 3265–3279.

Tytell, E. D., Hsu, C. Y., Williams, T. L., Cohen, A. H. and Fauci, L. J. (2010). Interactions between internal forces, body stiffness, and fluid environment in a neuromechanical model of lamprey swimming. *Proc. Natl. Acad. Sci. U. S. A.* **107**, 19832–19837.

van Ginneken, V., Antonissen, E., Müller, U. K., Booms, R., Eding, E. ., Verreth, J. and van den Thillart, G. (2005). Eel migration to the Sargasso: remarkably high swimming efficiency and low energy costs. *J. Exp. Biol.* **208**, 1329–1335.

Van Wassenbergh, S., Potes, N. Z., and Adriaens, D. (2015). Hydrodynamic drag constrains head enlargement for mouthbrooding in cichlids. *J. R. Soc. Interface* **12**, 20150461.

Wainwright, S. A., Vosburgh, F. and Hebrank, J. H. (1978). Shark skin: Function in locomotion. *Science (80-.).* **202**, 747–749.

Ward, A. B. and Brainerd, E. L. (2007). Evolution of axial patterning in elongate fishes. *Biol. J. Linn. Soc.* **90**, 97–116.

Watkins-Colwell, G., Love, K., Randall, Z., Boyer, D., Winchester, J., Stanley, E. and Blackburn, D. (2018). The Walking Dead: Status Report, Data Workflow and Best Practices of the oVert Thematic Collections Network. *Biodivers. Inf. Sci. Stand.* **2**, e26078.

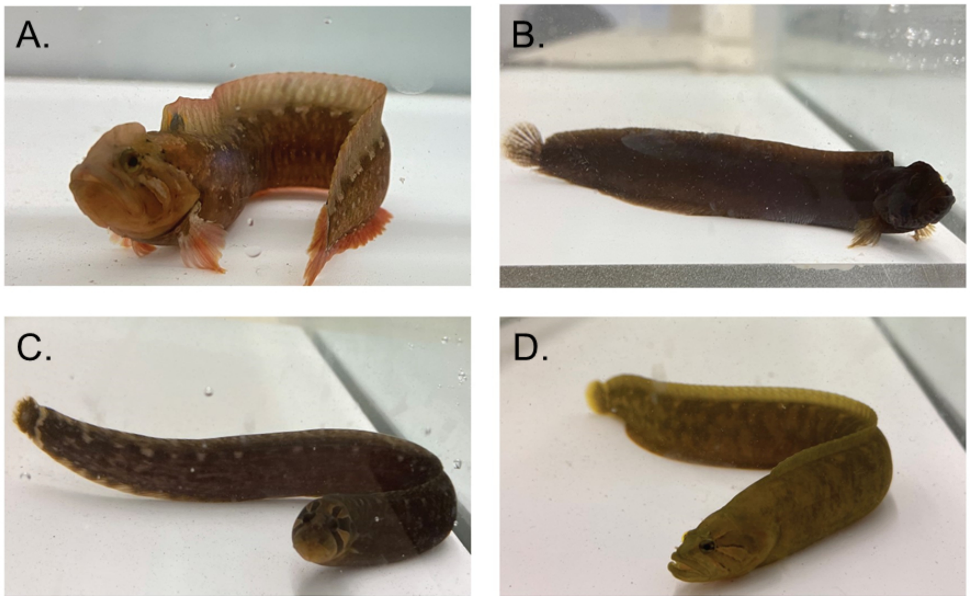

Figure 1. Four species of elongate fishes. A) *Anoplarchus purpurescens*. B) *Anoplarchus insignis*. C) *Xiphister atropurpureus*. D) *Xiphister mucosus*.

241x147mm (96 x 96 DPI)

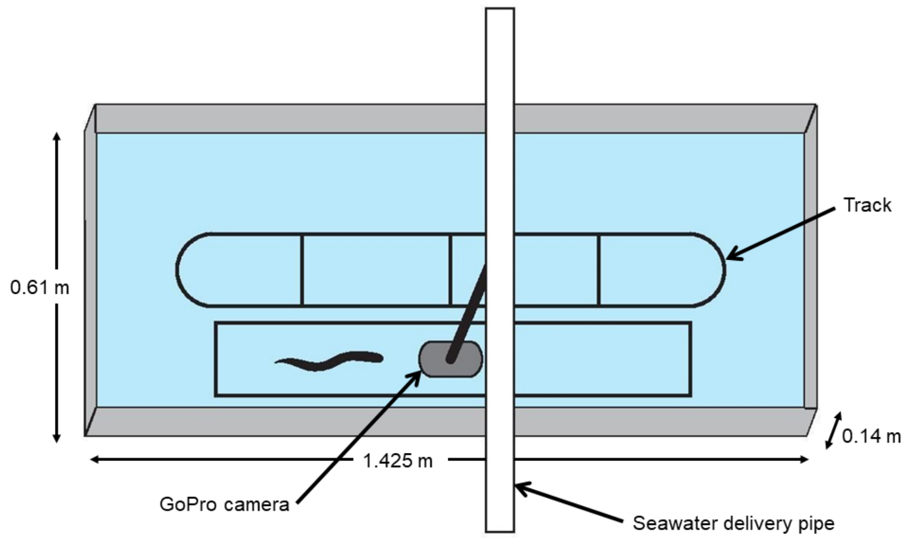

Figure 2. Video recording setup. Drawing shows an overhead view of the setup. Fishes swam around a track in the middle of the tank, crossing through the camera's field of view. The GoPro was suspended from the seawater delivery pipe above the tank.

279x165mm (96 x 96 DPI)

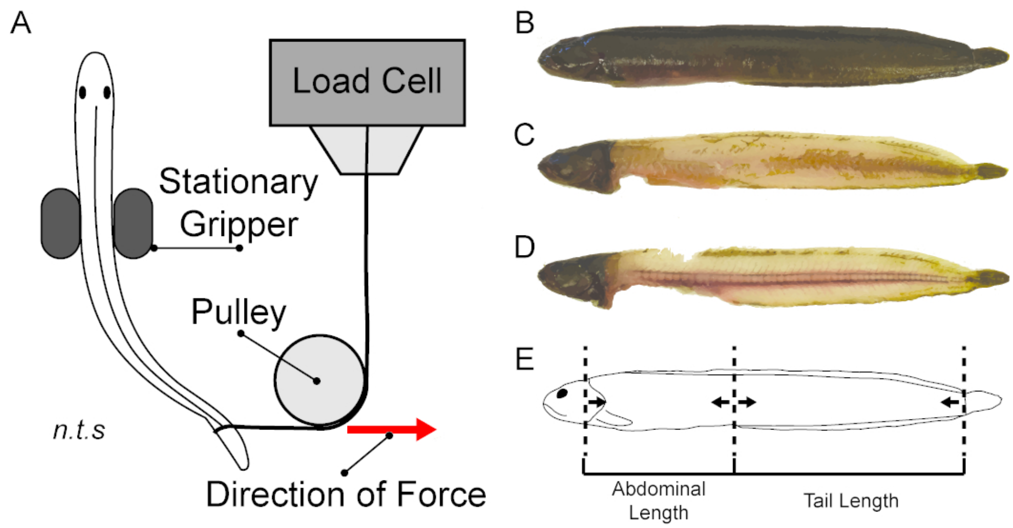

Figure 3. Mechanical testing method. A) Schematic of bending setup. This illustration shows a tail bending trial, where the stationary gripper is positioned at the anal fin and the pulling string is tied prior to the tail fin. The string was threaded through a pulley and the direction of force was maintained perpendicular to the body. B-D) Stages of dissection: B) whole fish, C) skin removed, and D) muscle removed. E) Defining regions for abdominal and tail bending tests. Arrows indicate the points of stationary gripper and string placement that are inward a distance of 10% of the region length.

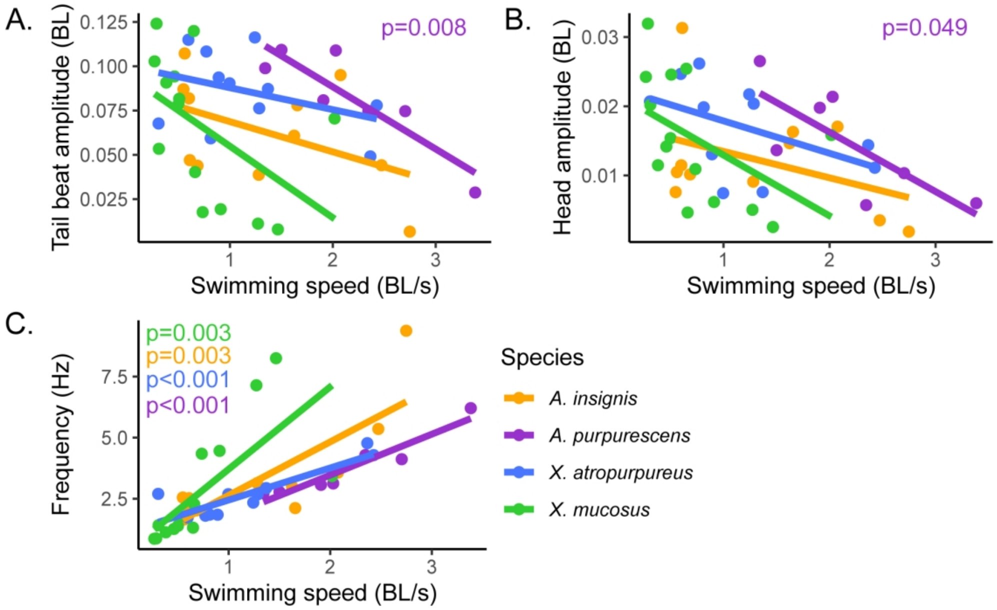

Figure 4. Varying swimming speed effect on wave properties of natural swimming kinematics. Each point represents one video recording trial of an individual fish. A) Average amplitude of tail movement in body lengths (BL) as a function of swimming speed in BL/second. B) Average amplitude of head movements as a function of swimming speed. C) Average tail beat frequency in hertz as a function of swimming speed. P values indicate a significant linear relationship between the variables for a particular species.

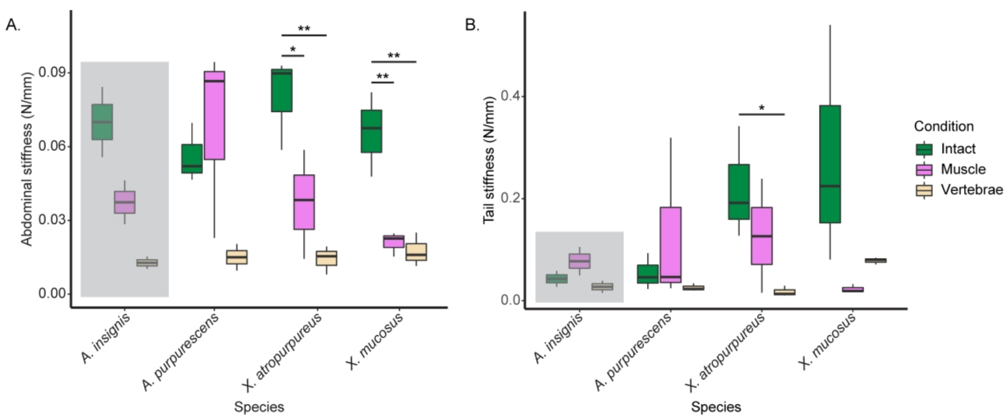

Figure 5. Stiffness of the abdominal and tail regions for each species under different dissection conditions. A) Stiffness (calculated as N/mm) of the abdominal region when bent fully intact, with skin removed to expose the muscle, and with muscle removed to expose the vertebral column. B) Stiffness of the tail region when bent in the three different material testing conditions. Post hoc comparisons are denoted by lines with stars above significantly different groups. Grey boxes over data for *A. insignis* indicate that no statistics were run on this species for material testing as there were only two individuals (N=2).

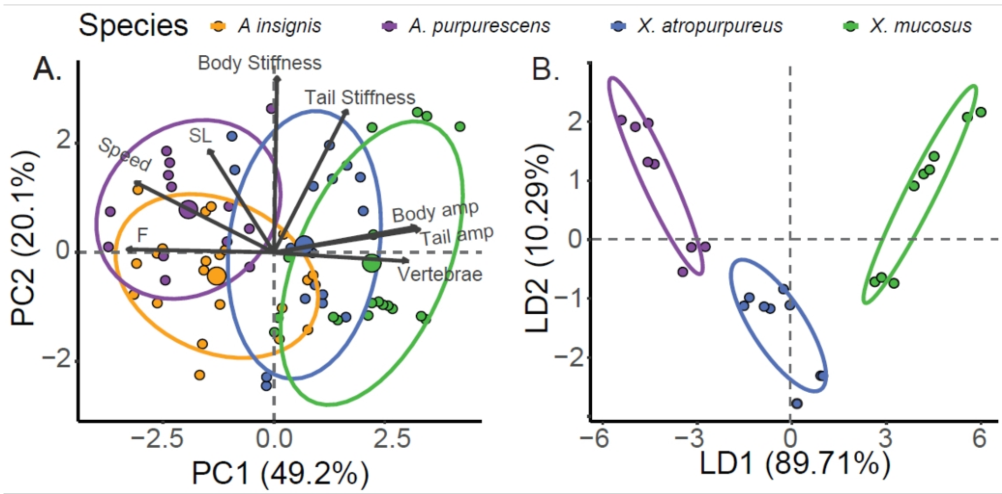

Figure 6. Principal component and linear discriminant plots of swimming kinematics, material testing, and vertebral counts obtained from CT scan scans. Percentages of PC axis show the percentage of variation explained by each PC. Percentages of LD axis show the percentage of between group variation described by the LD. Ellipses are drawn at a 75% confidence level using a multivariate t-distribution.

311x153mm (96 x 96 DPI)

Table 1. Specimens used in this study

Species	Specimens filmed	Specimens material tested	CT scans analyzed	Size range (cm)
Anoplarchus insignis	5	2	3	11-15.5
Anoplarchus purpurescens	5	3	4	8-15
Xiphister atropurpureus	5	3	4	8.5-19
Xiphister mucosus	5	3	4	11-25

Table 2. Merged kinematics and mechanics. Values shown are p-values. Bolded values are significant and italicized values are approaching significance.

Condition	Intact		Muscle Only		Bone Only	
Position	**Body**	**Tail**	**Body**	**Tail**	**Body**	**Tail**
Speed	0.618	0.878	**<0.001**	*0.088*	0.550	0.447
Frequency	0.769	0.778	0.490	0.294	0.498	0.414
Body Amplitude	0.609	0.824	0.396	0.126	0.336	0.223
Tail Amplitude	0.152	0.457	0.635	**0.039**	0.399	**0.013**

Table 3. Loadings for all three LDs. Bolded values indicate inputs which contribute most to each axis

	LD1	LD2
Tail Stiffness	-0.54521	-0.18259
Body Stiffness	0.368791	-0.00608
Swim Speed	**4.082834**	**6.046713**
Tail Beat Frequency	-2.77633	**-5.15873**
Stride Length	**-5.59385**	-3.28076
Body Amplitude	-0.68109	**-4.03552**
Tail Amplitude	1.863151	2.640358